1521-009X/43/2/208–216$25.00
Drug Metabolism and Disposition
http://dx.doi.org/10.1124/dmd.114.061812
Drug Metab Dispos 43:208–216, February 2015


# Characterization of CYP2B6 in a CYP2B6-Humanized Mouse Model: Inducibility in the Liver by Phenobarbital and Dexamethasone and Role in Nicotine Metabolism In Vivo [S]

Zhihua Liu, Lei Li, Hong Wu, Jing Hu, Jun Ma, Qing-Yu Zhang, and Xinxin Ding

*Wadsworth Center, New York State Department of Health, and School of Public Health, University at Albany, Albany, New York (Z.L., L.L., H.W., J.H., J.M., Q.-Y.Z., X.D.); and College of Nanoscale Science and Engineering, SUNY Polytechnic Institute, Albany, New York (X.D.)*

Received October 29, 2014; accepted November 18, 2014

## ABSTRACT

**The aim of this study was to further characterize the expression and function of human CYP2B6 in a recently generated CYP2A13/2B6/2F1-transgenic (TG) mouse model, in which CYP2B6 is expressed selectively in the liver. The inducibility of CYP2B6 by phenobarbital (PB) and dexamethasone (DEX), known inducers of CYP2B6 in human liver, was examined in the TG mice, as well as in TG/*Cyp2abfgs*-null (or "CYP2B6-humanized") mice. Hepatic expression of CYP2B6 mRNA and protein was greatly induced by PB or DEX treatment in both TG and TG/*Cyp2abfgs*-null mice. Function of the transgenic CYP2B6 was first studied using bupropion as a probe substrate. In PB-treated mice, the rates of hepatic microsomal hydroxybupropion formation (at 50 $\mu$M bupropion) were >4-fold higher in TG/*Cyp2abfgs*-null than in *Cyp2abfgs*-null mice (for both male and female mice); the rate difference was accompanied by a 5-fold higher catalytic efficiency in the TG/*Cyp2abfgs*-null mice and was abolished by an antibody to CYP2B6. The ability of CYP2B6 to metabolize nicotine was then examined, both in vitro and in vivo. The rates of hepatic microsomal cotinine formation from nicotine were significantly higher in TG/*Cyp2abfgs*-null than in *Cyp2abfgs*-null mice, pretreated with PB or DEX. Furthermore, systemic nicotine metabolism was faster in TG/*Cyp2abfgs*-null than in *Cyp2abfgs*-null mice. Thus, the transgenic CYP2B6 was inducible and functional, and, in the absence of mouse CYP2A and CYP2B enzymes, it contributed to nicotine metabolism in vivo. The CYP2B6-humanized mouse will be valuable for studies on in vivo roles of hepatic CYP2B6 in xenobiotic metabolism and toxicity.**

## Introduction

The human cytochrome P450 (P450) *CYP2B* gene subfamily consists of only one functional gene, *CYP2B6*, and a pseudogene, *CYP2B7P*, located on chromosome 19 between 19q12 and 19q13.2 (Yamano et al., 1989). CYP2B6 has a large number of substrates, including more than 60 clinically used drugs, such as the antitumor agents cyclophosphamide and ifosfamide, the antiretroviral drugs nevirapine and efavirenz, the smoking-cessation drug bupropion, and the anesthetic propofol (Mo et al., 2009). CYP2B6 also metabolizes many notable environmental toxicants, including aflatoxin B1, 4-(methylnitrosamino)-1-(3-pyridyl)-1-butanone, nicotine, and chlorpyrifos, and such endogenous compounds as arachidonic acid, lauric acid, estrone, and testosterone (Dicke et al., 2005; Mo et al., 2009; Turpeinen and Zanger, 2012).

CYP2B6 is preferentially expressed in human liver; its hepatic expression level shows a large interindividual variability (~100-fold) and accounts for a maximum of ~10% of total hepatic P450 content (Mimura et al., 1993; Shimada et al., 1994; Turpeinen and Zanger, 2012). Hepatic CYP2B expression is highly inducible in humans as well as in rodents; well known CYP2B inducers include phenobarbital (PB), PB-like compounds, and the synthetic glucocorticoid dexamethasone (DEX) (Wang and Negishi, 2003; Wang and Tompkins, 2008).

We recently reported the generation and initial characterization of a CYP2A13/2B6/2F1-transgenic (TG) mouse model (Wei et al., 2012). In this mouse model, whereas the *CYP2A13* and *CYP2F1* genes are expressed mainly in the respiratory tract, the *CYP2B6* transgene was mainly expressed in the liver. The aim of the present study was to determine whether the *CYP2B6* transgene can be induced by known CYP2B6 inducers (PB and DEX) and whether the transgenic CYP2B6 is functional toward known CYP2B6 substrates (bupropion and nicotine). Initial studies on CYP2B6 mRNA induction were performed using TG mice. For subsequent studies, to avoid potential interference by mouse CYP2B proteins/enzymes, we crossbred the TG mouse with a newly generated *Cyp2abfgs*-null mouse, in which all mouse genes in the *Cyp2abfgs* gene subfamilies are deleted (Li et al., 2014), and then studied CYP2B6 expression and function in the resultant TG/*Cyp2abfgs*-null (also known as CYP2B6-humanized) mice, with use of the *Cyp2abfgs*-null mouse as a control. Our results demonstrate that CYP2B6 is highly inducible by both PB and DEX in the liver of the CYP2B6-humanized mouse, that it is active toward both bupropion and nicotine, and that its expression could influence nicotine metabolism in vivo in the absence of mouse CYP2A and CYP2B enzymes.

This work was supported in part by the National Institutes of Health [Grants CA092596 and ES020867].

Z.L. and L.L. contributed equally to this work.

dx.doi.org/10.1124/dmd.114.061812.

[S] This article has supplemental material available at dmd.aspetjournals.org.

**ABBREVIATIONS:** ANOVA, analysis of variance; CAR, constitutive androstane receptor; DEX, dexamethasone; GAPDH, glyceraldehyde 3-phosphate dehydrogenase; HPLC, high-performance liquid chromatography; P450, cytochrome P450; PB, phenobarbital; PCR, polymerase chain reaction; TG, CYP2A13/2B6/2F1-transgenic.

## Materials and Methods

**Chemicals and Reagents.** Phenobarbital, dexamethasone, bupropion hydrochloride, (2*S*,3*S*)-hydroxybupropion hydrochloride, hydroxybupropion-$d_6$, (–)-cotinine, (–)-cotinine-methyl-$d_3$ (cotinine-$d_3$), (–)-nicotine hydrogen tartrate, and NADPH were purchased from Sigma-Aldrich (St. Louis, MO). All solvents (acetonitrile, methanol, and water) were of high-performance liquid chromatography (HPLC) grade (Thermo Fisher Scientific, Houston, TX).

**Animals and Treatments.** All studies with mice were approved by the Institutional Animal Care and Use Committee of the Wadsworth Center. TG mice, CYP2B6-humanized (TG/*Cyp2abfgs*-null) mice, and *Cyp2abfgs*-null mice, all on C57BL/6 background, were allowed free access to water and food. The CYP2B6-humanized mice were all hemizygous for the *CYP2B6* transgene [TG(+/−)/*Cyp2abfgs*(−/−)]. To induce CYP2B6 expression, mice were treated with three consecutive daily injections (intraperitoneal) of phenobarbital sodium (80 mg/kg per day, in saline) or dexamethasone (80 mg/kg per day, in corn oil). Mice in control groups received saline or corn oil alone. Mice were euthanized by $CO_2$ overdose at 24 hours after the last injection, and tissues were store at –80°C until use.

**Immunoblot Analysis.** Microsomal proteins were separated on NuPAGE Bis-Tris gels (10%) (Invitrogen, Carlsbad, CA). Immunoblot analysis was performed as described (Ding and Coon, 1990). The expression of human CYP2B6 protein was analyzed using a mouse anti-human CYP2B6 monoclonal antibody (BD Biosciences, Bedford, MA). Calnexin, a marker protein for the endoplasmic reticulum, was detected using a rabbit anti-human calnexin antibody (GenScript, Piscataway, NJ). The secondary antibody was peroxidase-labeled rabbit anti-mouse IgG or goat anti-rabbit IgG, and was detected with an enhanced chemiluminescence Western blotting detection reagent (GE Healthcare, Buckinghamshire UK). The intensity of the target band was determined using the Bio-Rad GS-710 Imaging Densitometer (Bio-Rad, Hercules, CA).

**RNA-Polymerase Chain Reaction Analysis.** Total RNA was prepared using Trizol reagent (Invitrogen) and stored at –80°C. Reverse transcription of RNA was carried out using the SuperScript III first-strand synthesis system (Invitrogen), with use of 5 $\mu$g of total RNA, pretreated with DNase I (Invitrogen) at room temperature for 15 minutes, and 0.5 $\mu$g of oligo(dT), in a final volume of 20 $\mu$l. Realtime polymerase chain reaction (PCR) was performed on an ABI StepOne Plus PCR system (Applied Biosystems, Foster City, CA), using SYBR Green PCR core reagent (Applied Biosystem), essentially as described previously (Zhang et al., 2007). Reactions were performed, in duplicate, in a total volume of 10 $\mu$l, with 2 $\mu$l of diluted (1:15) first-strand cDNA as template. Reactions were initiated at 50°C for 2 minutes (to allow degradation of any potential contaminating PCR products by the AmpErase UNG [Life Technologies, Grand Island, NY]), followed by denaturation at 95°C for 10 minutes, and then 45 cycles of amplifications (95°C for 15 seconds, 62°C for 1 minute). The final melting curve analysis was carried out at 95°C for 15 seconds, 60°C for 1 minute, and 95°C for 15 seconds. The following primers were used: GAPDH, forward 5′-tgtgaacggatttggccgta-3′ and reverse 5′-tcgctcctggaagatggtga-3′ (Wei et al., 2012); CYP2B6, forward 5′-cattcttccggggattatggtg-3′ and reverse 5′-cctcatagtggtcacagagaatcg-3′ (Rencurel et al., 2005); CYP3A11, forward 5′-ggatgagatcgatgaggctctg-3′ and reverse 5′-caggtattccatctccatcacagt-3′; CYP2B10, forward 5′-caggtgatcggctcacacc-3′ and reverse 5′-tgactgcatctgagtatggcatt-3′ (Pan et al., 2000).

**In Vitro Assays for Bupropion and Nicotine Metabolism.** Bupropion hydroxylase activity was determined essentially as described (Walsky and Obach, 2009). Incubation mixtures consisted of 0.2 mg of liver microsomal protein, 50 $\mu$M bupropion chloride, 50 mM potassium phosphate buffer (pH 7.4), 5 mM magnesium chloride, and 1 mM NADPH, in a total volume of 0.2 ml. Reactions were initiated at 37°C by addition of NADPH. NADPH was omitted in negative control reactions. For immunoinhibition experiments, 0–200 $\mu$g of anti-CYP2B6 monoclonal antibody or normal mouse IgG (Sigma-Aldrich) in 25 mM Tris-HCl buffer (pH 7.5) were preincubated on ice with 0.1 mg of liver microsomal protein for 20 minutes, prior to the addition of the other components to initiate the reaction. For analysis of enzyme kinetics, initial rates were determined over a range of 10–1000 $\mu$M bupropion.

All reactions were terminated after 20 minutes, by addition of 20 $\mu$l of an acidified internal standard solution (containing 3% formic acid and 20 pmol of hydroxybupropion-$d_6$); the mixtures were centrifuged, to precipitate protein, and the resultant supernatant was used for determination of hydroxybupropion, with use of an Agilent 1200 Series HPLC, fitted with a Phenomenex Gemini C18 column (50 × 2 mm, 5 $\mu$m) (Phenomenex, Torrance, CA), and an ABI 4000 QTRAP mass spectrometer (AB Sciex, Framingham, MA). For HPLC, the mobile phase [A: 5 mM aqueous ammonium formate, B: 95:5 acetonitrile/methanol (v/v), both containing 0.05% (v/v) formic acid] was delivered at a flow rate of 0.5 ml/min with the following program: 2% B for 0.5 minutes, linear gradient to 71% B between 0.5 and 3.7 minutes, linear gradient to 98% B between 3.7 and 3.9 minutes, held at 98% B until 4.5 minutes, linear gradient to 2% B between 4.5 and 4.6 minutes, then re-equilibrated to initial conditions between 4.6 and 8.0 minutes. Retention time for hydroxybupropion was 3.9 minutes. The mass spectrometer was operated in a positive ion mode with electrospray ionization source. The parent/product ion pairs of *m/z* 256/139 (for hydroxybupropion) and *m/z* 262/139 (for hydroxybupropion-$d_6$) were monitored in the multiple reaction monitoring scan mode. Authentic compound was used for matching retention times and mass spectrometry spectra, and as standard for quantification. The parameters for the chamber were as follows: curtain gas, 40 psig; heated nebulizer temperature, 350°C; ion spray voltage, 4000 V; nebulizer gas, 50 psig; turbo gas, 50 psig; declustering potential, 40 V; and entrance potential, 10 V. The calibration curve for hydroxybupropion was prepared by spiking authentic standard and internal standard to incubation mixtures containing boiled microsomes (recovery >85%).

Nicotine C-5′-oxidation was assayed essentially as described previously (Zhou et al., 2010). Reaction mixtures contained 1.0, 10, or 100 $\mu$M nicotine, 0.5 mg/ml liver microsomal protein, 1.0 mg/ml cytosolic protein (postmicrosomal fraction from livers of untreated wild-type mice), and 1 mM NADPH, in a total volume of 0.3 ml. Reactions were initiated at 37°C by addition of NADPH, and terminated after 15 minutes, by addition of 1 ml of ice-cold methanol (containing 1 ng of cotinine-$d_3$). The mixtures were centrifuged, and the resultant supernatant was dried under nitrogen, and then reconstituted with 50% (v/v) methanol in water, for measurement of cotinine, as described (Zhou et al., 2010).

**Pharmacokinetic Analysis for Nicotine.** Pharmacokinetic studies were performed as described (Zhou et al., 2010). Mice (male, $n$ = 3–4/group) were administrated with a single injection (at 9:00–10:00 AM) of nicotine tartrate (1.0 mg/kg i.p., free base) in saline. Blood was serially collected from the tail vein, at various times (5 minutes to 4 hours) after dosing. Cotinine-$d_3$ was added as internal standard. The plasma levels of nicotine and cotinine were determined by use of liquid chromatography–mass spectrometry (Zhou et al., 2010).

**Other Methods and Data Analysis.** Genotypic analysis for the TG mouse and the *Cyp2abfgs*-null mouse was performed as described (Wei et al., 2012; Li et al., 2014). Microsomes were prepared as described previously (Ding and Coon, 1990). Pharmacokinetic parameters were calculated by use of the noncompartmental method in the PKSolver software (Zhang et al., 2010). Enzyme kinetic parameters were calculated using GraphPad Prism (GraphPad, San Diego, CA); one-enzyme Michaelis-Menten equation was used for data analysis. Statistical significance of differences between two groups in various parameters was examined using Student's $t$ test or with two-way analysis of variance (ANOVA), followed by Bonferroni post-test, using GraphPad Prism.

## Results

**Effects of PB and DEX on *CYP2B6* Transgene Expression.** To determine whether hepatic expression of transgenic CYP2B6 can be regulated by PB and DEX as in human hepatocytes, we measured hepatic CYP2B6 mRNA and protein levels in TG and/or TG/*Cyp2abfgs*-null mice, at 24 hours following three daily injections of PB or DEX [each at 80 mg/kg per day i.p., a commonly used dose for induction of CYP2B (Zhang et al., 2003; Pustylnyak et al., 2007)] or the corresponding vehicle. Initial studies were performed using male TG mice; as shown in Fig. 1, A and B, the levels of transgenic CYP2B6 mRNA, as well as that of mouse CYP2B10 mRNA (as a positive control), were remarkably increased by both PB and DEX. The level of mouse CYP3A11 mRNA was also increased by DEX, and minimally by PB, treatment, as expected (Zhang et al., 2003).

In TG/*Cyp2abfgs*-null mice, PB and DEX induced hepatic CYP2B6 protein expression in both males and females; however, the induced level by either inducer was 2–3 times greater in males than in females (Fig. 1, C and D). In vehicle-treated TG/*Cyp2abfgs*-null mice, CYP2B6 was barely detected in the liver, and a significant sex difference in basal levels of CYP2B6 expression could not be established with confidence because of the low amounts (Fig. 1, C and D). The inducibility by PB and DEX, as well as the sex difference in the levels achieved by the induction, was confirmed in studies with male and female TG mice (Supplemental Fig. 1). In additional studies not presented, hepatic expression of mouse CYP2B, 2C, and 3A proteins was also induced by PB and DEX in the TG mice, as expected (data not shown).

In experiments not shown, we did not detect CYP2B6 protein in extrahepatic tissues of PB-treated TG mice, including brain, kidney, lung, nasal mucosa, small intestine, and testis (with an estimated detection limit of ~25 fmol/mg microsomal protein). Furthermore, in the lung, where the other two transgenes, *CYP2A13* and *CYP2F1*, are expressed (Wei et al., 2012), the expression of CYP2A13 and CYP2F1 was not increased by PB or DEX.

**Hepatic Microsomal CYP2B6 Activity toward Bupropion.** To demonstrate that transgenic CYP2B6 protein is functional, we compared hepatic microsomal activity toward bupropion, a selective CYP2B substrate (Faucette et al., 2000), between TG/*Cyp2abfgs*-null and *Cyp2abfgs*-null mice, treated with either saline or PB. It was necessary to study CYP2B6 activity on a *Cyp2b*-null background given the high activity of mouse CYP2B enzymes toward bupropion. As shown in Fig. 2A, in control (saline-treated) mice, the bupropion hydroxylase activity was not different between TG/*Cyp2abfgs*-null and *Cyp2abfgs*-null mice, for either male or female, although this basal activity appeared to be slightly (<2-fold) higher in males than in females, for both *Cyp2abfgs*-null mice and TG/*Cyp2abfgs*-null mice (not statistically significant according to two-way ANOVA/Bonferroni post-test). The absence of a significant difference between TG/*Cyp2abfgs*-null mice and *Cyp2abfgs*-null mice suggested that constitutively expressed CYP2B6 did not make a significant contribution to

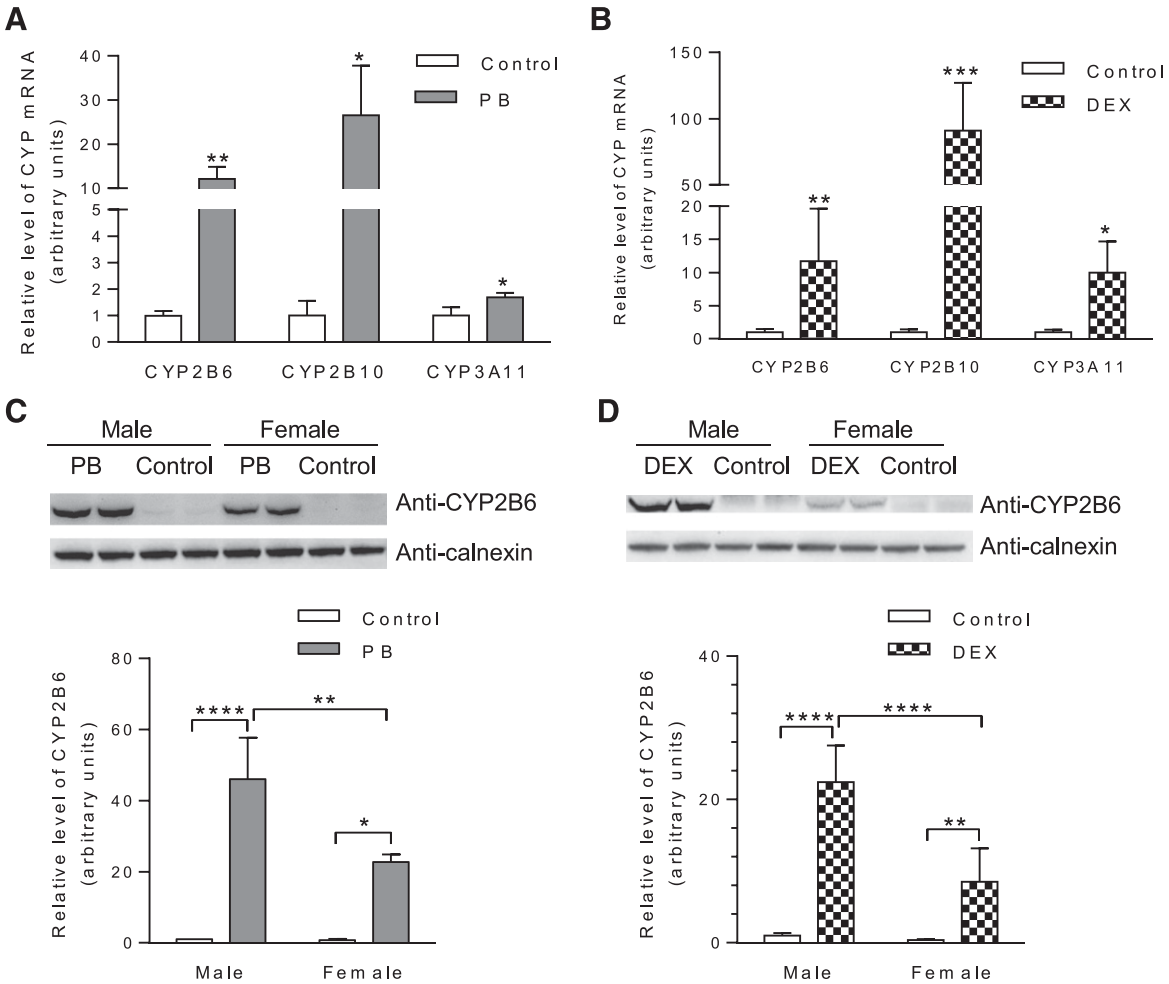


**Fig. 1.** Effects of PB and DEX on hepatic expression of transgenic CYP2B6. (A and B) Induction of hepatic CYP2B6 mRNA expression by PB and DEX in TG mice. Mice (male, hemizygous, 2-month-old) were treated with PB [80 mg/kg per day (A)] or DEX [80 mg/kg per day (B)], or corresponding vehicle (saline or corn oil, respectively), by intraperitoneal injection, once daily for 3 consecutive days. Livers from individual mice were obtained 24 hours after the last dose for RNA isolation and PCR analysis of relative levels of CYP2B6 as well as mouse CYP2B10 and CYP3A11. Data represent means ± S.D. ($n$ = 3–4) and were normalized by the levels of GAPDH. (C and D) Induction of hepatic CYP2B6 protein expression by PB and DEX in CYP2B6-humanized mice. Mice (male or female, 2-month-old) were treated with PB (C) or DEX (D), or with corresponding vehicles (as described above). Livers were obtained 24 hours after the last dose for microsome preparation and immunoblot analysis. Microsomal proteins prepared from pooled tissues from 3–4 mice (40 $\mu$g per lane, PB-treated; 80 $\mu$g per lane, DEX-treated) were analyzed in duplicate, with use of an anti-CYP2B6 monoclonal antibody. Calnexin was detected as a loading control. Typical results are shown on top and results of quantitative analysis for three different sets of microsomes are shown below; data represent means ± S.D. ($n$ = 3), and were normalized by the levels of calnexin. *$P < 0.05$; **$P < 0.01$; ***$P < 0.001$; ****$P < 0.0001$; statistical significance was assessed using unpaired $t$ test (A and B) or two-way ANOVA with Bonferroni post-test (C and D).

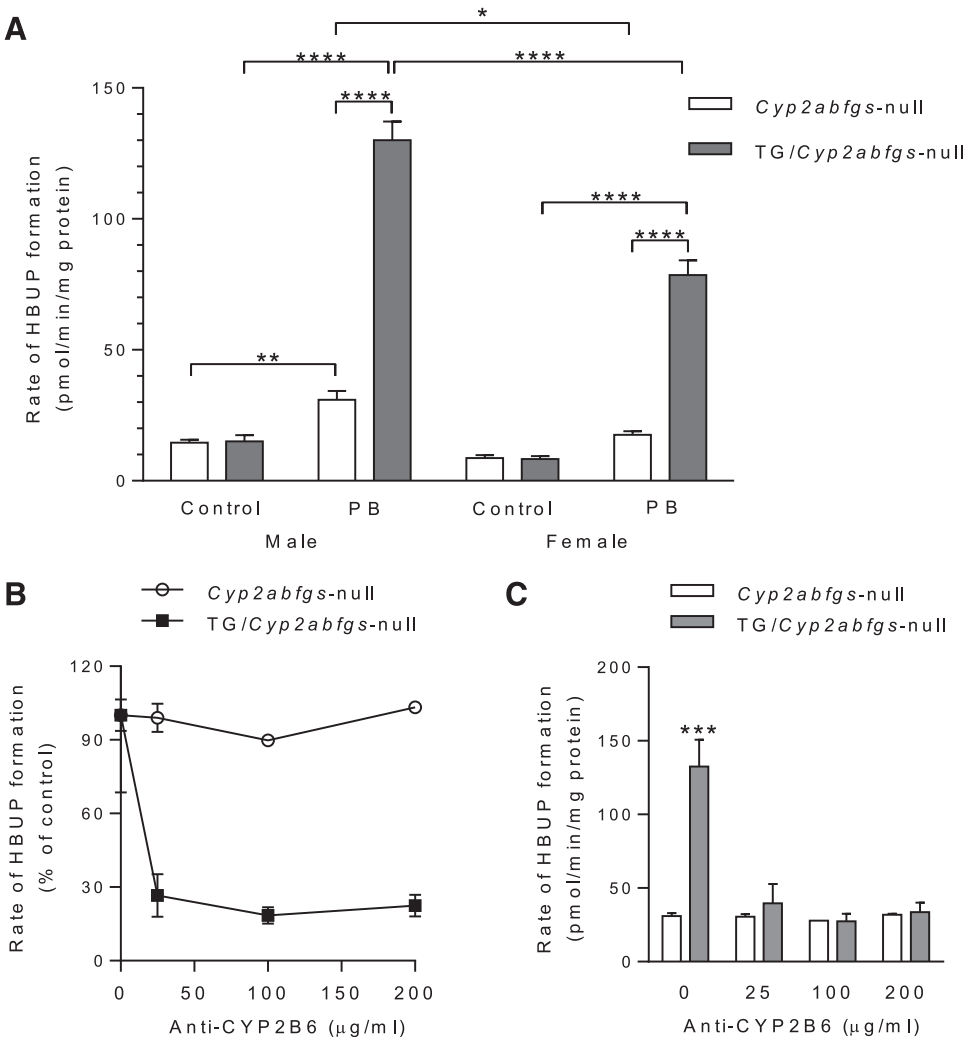


**Fig. 2.** Activity of transgenic CYP2B6 toward bupropion hydroxylation. (A) Bupropion hydroxylase activity in hepatic microsomes from saline or PB-treated TG/*Cyp2abfgs*-null and *Cyp2abfgs*-null mice. Mice (2-month-old, male and female) were treated with PB or saline as described in Fig. 1A. Rates of formation of hydroxybupropion (HBUP) were determined in reaction mixtures containing 50 mM potassium phosphate buffer, pH 7.4, 50 $\mu$M bupropion, 5 mM magnesium chloride, 1 mg/ml liver microsomal protein, and 1.0 mM NADPH. Values represent means ± S.D. ($n$ = 3–4). $^{*}P < 0.05$; $^{**}P < 0.001$, $^{****}P < 0.0001$; two-way ANOVA with Bonferroni post-test. (B and C) Inhibition by anti-CYP2B6. Liver microsomes from PB-treated, male, *Cyp2abfgs*-null and TG/*Cyp2abfgs*-null mice (0.5 mg protein per milliliter) were preincubated with various amounts of anti-CYP2B6 (0–200 $\mu$g protein/ml) before initiation of reaction. Results are shown either as percentages of the control activity (B) or as rates (C). Data represent means ± S.D. ($n = 3$). $^{***}P < 0.001$, compared with corresponding null group (two-way ANOVA with Bonferroni post-test).

total microsomal bupropion hydroxylase activity, at the substrate concentration tested.

PB treatment induced bupropion hydroxylase activity in both male (2.1-fold) and female (2.0-fold) *Cyp2abfgs*-null mice (though the female data did not reach statistical significance according to two-way ANOVA), as well as in both male (8.6-fold) and female (9.4-fold) TG/*Cyp2abfgs*-null mice. Importantly, following PB treatment, activity was significantly higher in TG/*Cyp2abfgs*-null mice than in *Cyp2abfgs*-null mice, 4.2-fold in males and 4.5-fold in females, indicating substantial contribution of CYP2B6 to total microsomal activity. Consistent with the sex difference in induced levels of CYP2B6 protein in liver microsomes, the induced activity was also significantly greater (~1.5-times) in male than in female TG/*Cyp2abfgs*-null mice (Fig. 2A). Notably, bupropion hydroxylase activity in PB-treated *Cyp2abfgs*-null mice was also significantly greater (~1.5-times) in males than in females.

The contribution of transgenic CYP2B6 to hepatic microsomal bupropion hydroxylation was further determined in an immunoinhibition assay, with use of the monoclonal anti-CYP2B6 antibody (Fig. 2, B and C). Addition of the anti-CYP2B6 antibody at various concentrations (0-200 $\mu$g/ml) led to ~80% maximal inhibition of bupropion hydroxylation in microsomes from PB-treated male TG/*Cyp2abfgs*-null mice, assayed at 50 $\mu$M bupropion. No inhibition was observed in microsomes from PB-treated *Cyp2abfgs*-null mice, a result confirming specificity of the antibody. As an additional control, addition of normal (preimmune) IgG at 200 $\mu$g/ml did not cause any inhibition of the activity in either mouse strain (data not shown). Notably, as shown in Fig. 2C, rates of residual bupropion hydroxylase activity in microsomes from TG/*Cyp2abfgs*-null mice incubated with saturating amounts of anti-CYP2B6 antibody were identical to that of *Cyp2abfgs*-null mice, indicating that the antibody inhibition of CYP2B6 activity was complete, and further confirming that the activity difference between the two strains was caused by the expression and induction of the transgenic CYP2B6.

Kinetic parameters for liver microsomal bupropion hydroxylation were determined using microsomes from PB-treated mice, over a substrate concentration range of 10–1000 $\mu$M (substrate-velocity curves are shown in Fig. 3A). Further analysis of the activity data on Eadie-Hofstee plots (Fig. 3B) revealed a single kinetic component in both samples. The apparent $K_m$ values were 146 ± 12 $\mu$M for the *Cyp2abfgs*-null mice and 119 ± 9 $\mu$M for the TG/*Cyp2abfgs*-null mice ($P < 0.05$, compared with null; $n = 3$), whereas the apparent $V_{max}$ values were 69 ± 2 pmol/min per milligram for the *Cyp2abfgs*-null mice and 267 ± 7 pmol/min per milligram for the TG/*Cyp2abfgs*-null mice ($P < 0.001$, compared with null); the calculated catalytic efficiency ($V_{max}/K_m$) was ~5-times greater for the TG/*Cyp2abfgs*-null mice (2.26 ± 0.12 $\mu$l/min per milligram) than for the *Cyp2abfgs*-null mice (0.47 ± 0.05 $\mu$l/min per milligram) ($P <$ 0.001, compared with *Cyp2abfgs*-null).

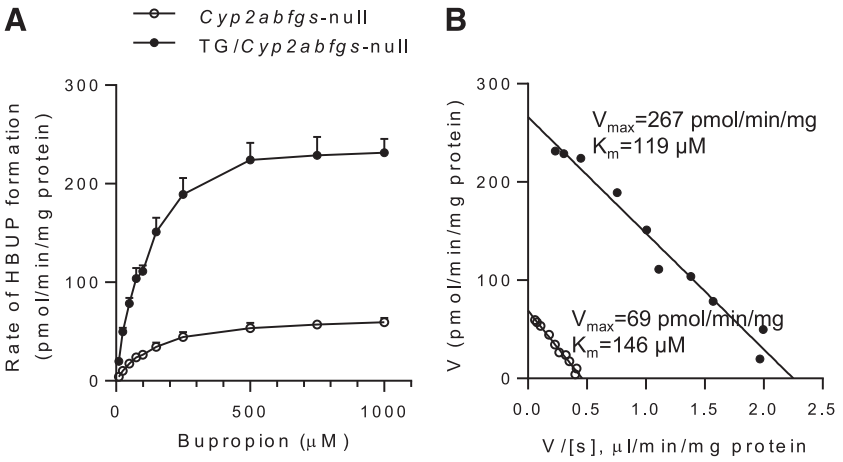


**Fig. 3.** Enzyme kinetic analysis of hepatic microsomal activity toward bupropion hydroxylation. Rates of liver microsomal HBUP formation were determined for PB-treated, female TG/*Cyp2abfgs*-null and *Cyp2abfgs*-null mice (2-month-old), as described in Fig. 2, with bupropion at 10–1000 $\mu$M, and shown as both substrate-velocity curves (A) and Eadie-Hofstee plots (B). The values in (A) represent means ± S.D. ($n$ = 3). Apparent $K_m$ values: 146 ± 12 $\mu$M for *Cyp2abfgs*-null; 119 ± 9 $\mu$M for TG/*Cyp2abfgs*-null. Apparent $V_{max}$ values: 69 ± 2 pmol/min per milligram for *Cyp2abfgs*-null, 267 ± 7 pmol/min per milligram for TG/*Cyp2abfgs*-null. Catalytic efficiency ($V_{max}/K_m$): 0.47 ± 0.05 $\mu$l/min per milligram for *Cyp2abfgs*-null, 2.26 ± 0.12 $\mu$l/min per milligram for TG/*Cyp2abfgs*-null.

**Hepatic Microsomal CYP2B6 Activity toward Nicotine.** To further characterize function of the transgenic CYP2B6, we measured liver microsomal nicotine oxidase activity for *Cyp2abfgs*-null mice and TG/*Cyp2abfgs*-null mice (2-month-old, male), treated with PB or DEX to induce CYP2B6. Two nicotine concentrations (1 and 10 $\mu$M) were initially examined, as described earlier in a study on wild-type and *Cyp2a5*-null mice (Zhou et al., 2010). As shown in Fig. 4, PB or DEX treatment led to significant increases in rates of cotinine formation in the TG/*Cyp2abfgs*-null mice, at either 1 or 10 $\mu$M nicotine. In contrast, PB or DEX treatment did not lead to significant increases in rates of cotinine formation in the *Cyp2abfgs*-null mice. Further, the rates in PB- or DEX-treated TG/*Cyp2abfgs*-null mice were all significantly higher than rates in corresponding PB- or DEX-treated null mice. Additionally, at either 1 $\mu$M or 10 $\mu$M nicotine, the presence of basal levels of CYP2B6 in the TG/*Cyp2abfgs*-null mice was not associated with significant increases in rates of nicotine oxidation, indicating that constitutively expressed CYP2B6 did not make a significant contribution to total microsomal activity at these nicotine concentrations tested.

The microsomal samples from *Cyp2abfgs*-null and TG/*Cyp2abfgs*-null mice (control or PB-treated) were further analyzed for nicotine oxidase activity at an even higher nicotine concentration (100 $\mu$M) (Fig. 4A). At this substrate concentration, a small (~30%) but significant increase in activity was observed in vehicle-treated TG/*Cyp2abfgs*-null mice, compared with vehicle-treated *Cyp2abfgs*-null mice, indicating CYP2B6 activity. Additionally, PB treatment led to a ~50% increase in activity in the *Cyp2abfgs*-null mice, in contrast to a ~5-fold increase in activity in the TG/*Cyp2abfgs*-null mice.

**Impact of Transgenic CYP2B6 Expression on Nicotine and Cotinine Pharmacokinetics.** To determine the role of transgenic CYP2B6 in drug metabolism in vivo, we conducted a pharmacokinetic study for nicotine and its metabolite cotinine in TG/*Cyp2abfgs*-null mice and *Cyp2abfgs*-null mice. Control or PB-pretreated mice (3-month-old, male) were given an injection of nicotine at 1 mg/kg i.p., a dose routinely used for pharmacokinetic studies on nicotine [e.g., Zhou et al. (2010)]. As shown in Fig. 5A, in the vehicle-treated control group, plasma nicotine levels were slightly higher in the *Cyp2abfgs*-null mice than in TG/*Cyp2abfgs*-null mice, whereas plasma cotinine levels were clearly higher in the TG/*Cyp2abfgs*-null mice than in the *Cyp2abfgs*-null mice. Pharmacokinetic analysis of the data in Fig. 5A indicated a relatively small, but statistically significant difference in clearance rate (CL/F) for plasma nicotine between TG/*Cyp2abfgs*-null (2.5 ± 0.4 ml/min) and *Cyp2abfgs*-null groups (1.4 ± 0.6 ml/min), and in $AUC_{0-240min}$ and $C_{max}$ values for plasma cotinine (Table 1). These data indicated that constitutively expressed transgenic CYP2B6 had a small, though significant, role in nicotine clearance and a much larger role in cotinine formation, in vivo.

Further pharmacokinetics studies on PB-treated TG/*Cyp2abfgs*-null and *Cyp2abfgs*-null mice (Fig. 5B) showed that, at the induced level, CYP2B6 played a more substantial role in nicotine clearance as well as cotinine formation in vivo. Nicotine clearance rate was significantly higher in PB-treated TG/*Cyp2abfgs*-null mice (3.1 ± 0.3 ml/min) than in PB-treated *Cyp2abfgs*-null mice (1.6 ± 0.1 ml/min); the increase in clearance rates was accompanied by ~40% decreases in $C_{max}$ and AUC values in PB-treated TG/*Cyp2abfgs*-null mice compared with PB-treated *Cyp2abfgs*-null mice (Table 1). Consistent with the increased nicotine clearance, plasma cotinine levels were substantially higher in PB-treated TG/*Cyp2abfgs*-null mice than in PB-treated *Cyp2abfgs*-null mice, as indicated by 3- to 4-fold increases in $C_{max}$ and AUC values (Table 1).

In *Cyp2abfgs*-null mice, there was no significant difference in nicotine clearance or cotinine formation between the PB-treated and vehicle-treated groups (Table 1), which is consistent with the results from in vitro studies (Fig. 4A), and indicated that the residual mouse P450s that are also induced by PB did not contribute to nicotine clearance at the dose tested. In TG/*Cyp2abfgs*-null mice, the AUC value for nicotine was significantly decreased, whereas the AUC value for cotinine was significantly increased, in PB-treated compared with vehicle-treated groups (Table 1), further confirming induction of transgenic CYP2B6 by PB.

## Discussion

Whereas the in vitro function and regulation of CYP2B6 can be readily studied using recombinant CYP2B6 enzyme, human liver microsomes, and cultured human primary hepatocytes, the in vivo impact of hepatic CYP2B6 expression or induction on drug metabolism, drug efficacy, drug-drug interaction, and drug/xenobiotic toxicity is more difficult to assess. This difficulty may result from the large interindividual variations in CYP2B6 expression and from the complex interplay between pharmacokinetics and pharmacodynamics, between effects of the parent drug and those of its metabolites, between metabolism and transport, and between endogenous regulators and drug inducers. Thus, an animal model with constitutive as well as inducible hepatic expression of human CYP2B6, such as the CYP2B6-humanized mouse model described in the present study, will be very useful for a variety of applications, including identification of chemical compounds and pathologic conditions that may alter CYP2B6 expression under in vivo conditions, validation or prediction of clinical drug-drug

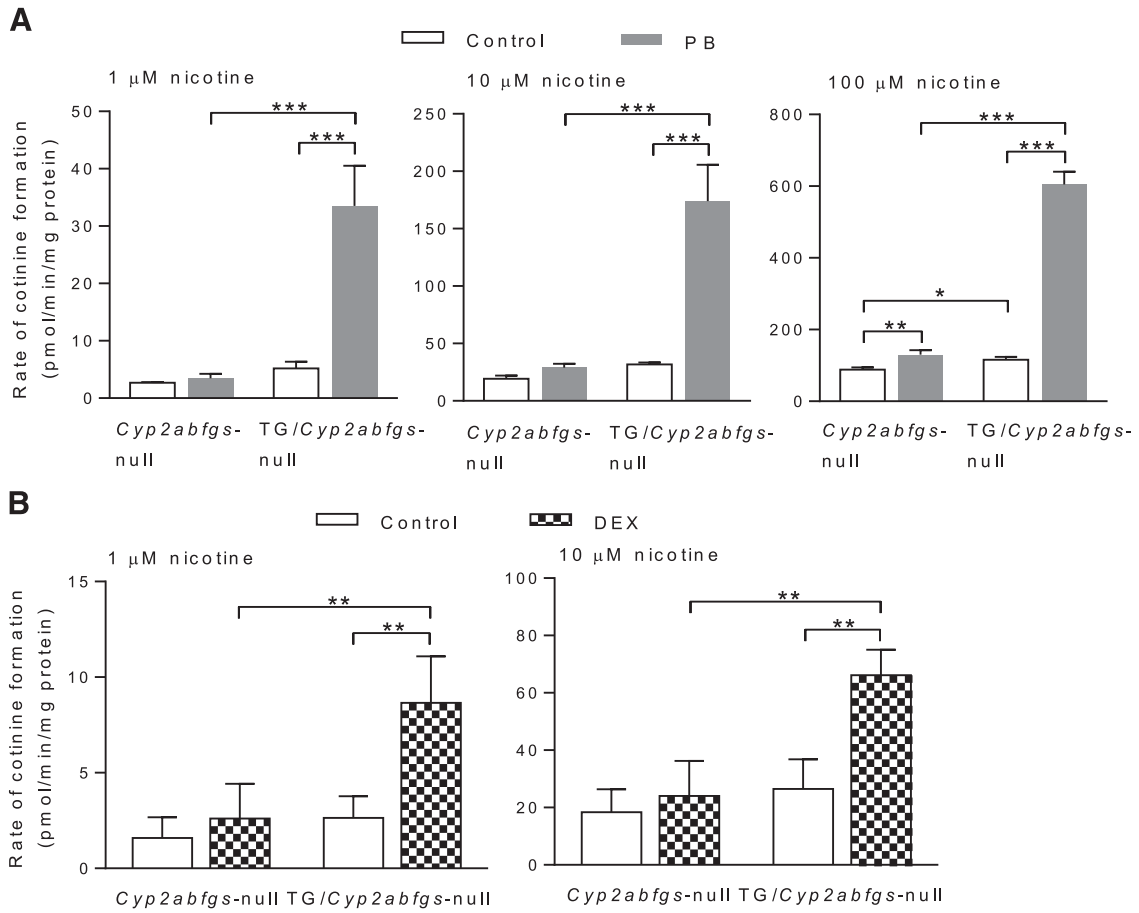


**Fig. 4.** Activity of transgenic CYP2B6 toward nicotine oxidation. Hepatic microsomes from PB- (A), DEX- (B), or corresponding vehicle-treated TG/*Cyp2abfgs*-null and *Cyp2abfgs*-null mice (2-month-old, male) were assayed for rates of cotinine formation from nicotine. Reaction mixtures contained 50 mM potassium phosphate buffer, pH 7.4, 1.0, 10, or 100 $\mu$M nicotine (as indicated), 0.5 mg/ml liver microsomal protein, and 1.0 mg/ml liver cytosol protein (as a source of aldehyde oxidase) from (untreated) 2-month-old male wild-type mice, and 1.0 mM NADPH. Values represent means ± S.D. ($n = 3$). *$P < 0.05$; **$P < 0.01$; ***$P < 0.001$ (two-way ANOVA with Bonferroni post-test).

interactions, identification of in vivo CYP2B6 drug metabolites that mediate drug efficacy or toxicity, and determination of the ability of hepatic CYP2B6 to mediate chronic diseases, such as cancer, that are caused by xenobiotic exposure, such as cigarette smoking.

As a first application of the CYP2B6-humanized mouse model, we examined the role of CYP2B6 in nicotine metabolism in vivo. Whereas CYP2A6 is the main, high-affinity enzyme for nicotine metabolism in human liver, CYP2B6 can also metabolize nicotine (Yamazaki et al., 1999). The contribution of CYP2B6 to nicotine clearance in humans is believed to be relatively small and influenced by the activity of the more dominant CYP2A6 (Yamanaka et al., 2004; Dicke et al., 2005; Al Koudsi and Tyndale, 2010). The impact of CYP2B6 genetic polymorphisms on nicotine clearance has been examined in a number of studies, yielding positive results in some (Johnstone et al., 2006; Ring et al., 2007; Bloom et al., 2013), but not in others (Lee et al., 2007; Binnington et al., 2012). Here, we have provided in vivo proof-of-principle in the mouse model that CYP2B6 could make a significant contribution to nicotine oxidation and systemic clearance, particularly at the induced level, albeit in the absence of the more dominant mouse CYP2A5 and CYP2B enzymes.

The role of mouse CYP2A and 2B enzymes in nicotine metabolism and nicotine's pharmacological effects and behavioral responses were demonstrated recently using a *Cyp2a(4/5)bgs*-null mouse model (Li et al., 2013). In the present study, the lack of a substantial induction by PB or DEX of nicotine oxidase activity in the *Cyp2abfgs*-null mice supports the notion that the residual mouse P450s that are also induced by PB or DEX in the *Cyp2abfgs*-null mice, including CYP3A and CYP2C (Fig. 1A and data not shown), were not very active toward nicotine, at least at the relatively low nicotine concentrations tested. This result also confirms that the PB- or DEX-induced increases in rates of hepatic microsomal nicotine metabolism in the CYP2B6-humanized mice were not confounded by possible contributions of the residual mouse P450 enzymes.

In contrast to nicotine, rates of bupropion metabolism in *Cyp2abfgs*-null mice were induced by PB, and both basal and induced levels showed a trend of sex difference (higher in males; Fig. 2A). Notably, whereas CYP2B enzymes play a major role in bupropion hydroxylation, other P450 enzymes, including CYP2C and CYP2E1, have been found to have low activity levels toward bupropion (Faucette et al., 2000; Chen et al., 2010; Pekthong et al., 2012; Zhu et al., 2014). However, the induction and sex difference of these non-CYP2B6 activities do not account for the sex difference in bupropion hydroxylase activities seen in the CYP2B6-humanized mice (Fig. 2A), because the overall activity in the humanized mice was much higher.

The sex difference in the induced level of CYP2B6 protein (Fig. 1, C and D), as well as in microsomal CYP2B6 activity toward the probe drug bupropion, is robust and reproducible. The molecular basis of this sex difference is not clear. It may reflect potential sex differences in the expression or activity of the nuclear receptors that mediate CYP2B6 induction by PB (via constitutive androstane receptor, or

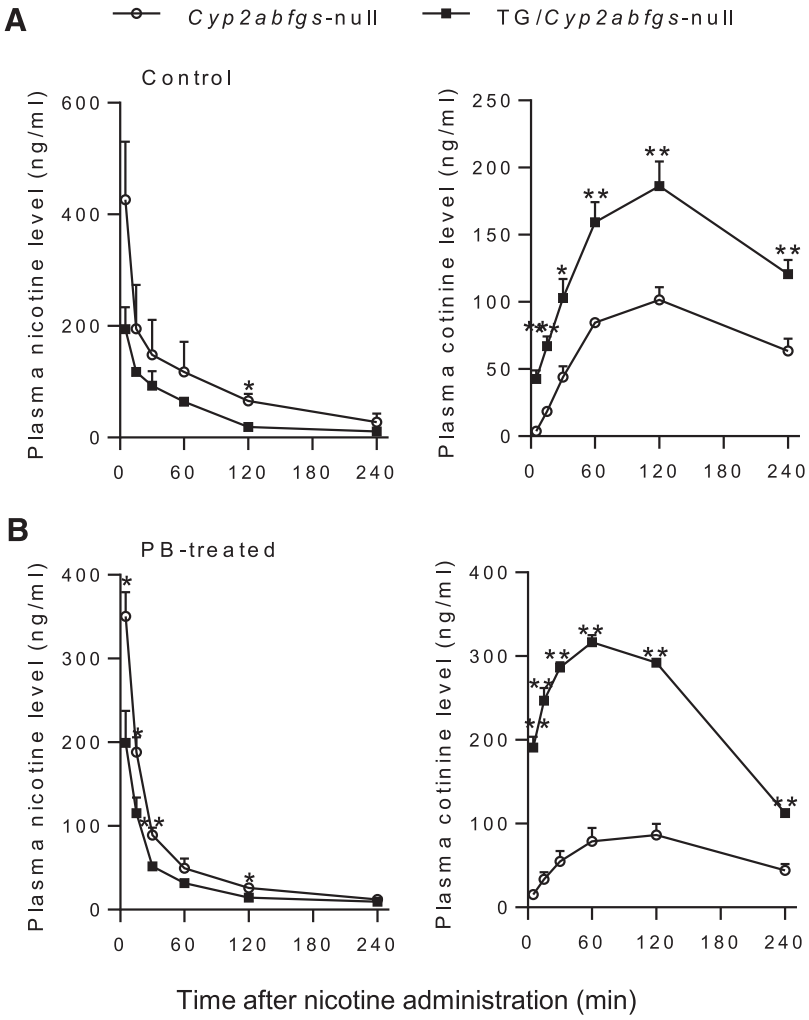


**Fig. 5.** Concentration-time curves for plasma nicotine and cotinine. TG/*Cyp2abfgs*-null and *Cyp2abfgs*-null mice (3-month-old, male) were treated with vehicle (A) or PB (B), as described in Fig. 1, and then, at 24 hours after the last treatment, were given nicotine at 1 mg/kg i.p. Plasma levels of nicotine and cotinine were determined at various times after nicotine injection. Data represent means ± S.E.M. ($n$ = 3–4). *$P < 0.05$; **$P < 0.01$, compared with *Cyp2abfgs*-null mice (Student's $t$ test)

CAR) and DEX [via glucocorticoid receptor, acting through CAR or pregnane X receptor (Wang et al., 2003)] in the CYP2B6-humanized mouse. It may also be attributable to potential sex differences in the metabolic disposition of the chemical inducers. Additionally, CYP2B6 expression is known to be stimulated by estrogen (Koh et al., 2012; Dickmann and Isoherranen, 2013), which also activates CAR (Kawamoto et al., 2000). Therefore, sex differences in hepatic estrogen homeostasis and/or estrogen receptor status might also have contributed to the observed sex difference in induced CYP2B6 levels in this mouse model. Future clarification of these potential mechanisms may help with predicting possible sex differences in CYP2B6 inducibility in human liver. In that regard, sex differences in liver CYP2B6 expression have been found in some studies [e.g., Lamba et al. (2003); Al Koudsi and Tyndale (2010)], but not in others [for a recent review, see Zanger and Klein (2013)], and may not reflect inherent differences in inducibility. Sexual dimorphism in CYP2B induction has been reported for certain strains of rats and mice (Waxman et al., 1985; Yamazoe et al., 1987; Corcos, 1992; Honkakoski et al., 1992). For example, in rats, CYP2B expression was induced by PB in males but not females in the Wistar strain, although it was induced in both males and females in the Fischer

TABLE 1

Pharmacokinetic parameters for plasma nicotine and cotinine in TG/*Cyp2abfgs*-null and *Cyp2abfgs*-null mice

Data from Fig. 5 were used for calculation of pharmacokinetic parameters. Values shown represent means ± S.D. ($n$ = 3–4).

| Analyte | Animals | $t_{1/2}$ | $T_{max}$ | $C_{max}$ | $AUC_{0-240min}$ | CL/F |
|---|---|---|---|---|---|---|
| | | *min* | | *ng/ml* | *ng·h/ml* | *ml/min* |
| Nicotine | *Cyp2abfgs-null*, vehicle-treated | 94 ± 50 | 5 ± 0 | 426 ± 181 | 364 ± 195 | 1.4 ± 0.6 |
| | TG/*Cyp2abfgs*-null, vehicle-treated | 77 ± 53 | 5 ± 0 | 173 ± 52 | 171 ± 18 | 2.5 ± 0.4* |
| Cotinine | *Cyp2abfgs-null*, vehicle-treated | N/A | 120 ± 0 | 102 ± 16 | 300 ± 39 | N/A |
| | TG/*Cyp2abfgs*-null, vehicle-treated | N/A | 120 ± 0 | 186 ± 32* | 577 ± 96** | N/A |
| Nicotine | *Cyp2abfgs-null*, PB-treated | 103 ± 62 | 5 ± 0 | 350 ± 51 | 205 ± 32 | 1.6 ± 0.1 |
| | TG/*Cyp2abfgs*-null, PB-treated | 84 ± 19 | 5 ± 0 | 199 ± 76* | 123 ± 9** | 3.1 ± 0.3** |
| Cotinine | *Cyp2abfgs-null*, PB-treated | N/A | 120 ± 0 | 87 ± 23 | 263 ± 79 | N/A |
| | TG/*Cyp2abfgs*-null, PB-treated | N/A | 60 ± 0** | 317 ± 17** | 971 ± 27** | N/A |

N/A, not applicable; *$P < 0.05$, **$P < 0.01$, compared with corresponding *Cyp2abfgs*-null value

344 strain (Larsen et al., 1994); this sexual dimorphism was found to be related to a strain-specific difference in the expression of CAR in the livers of the Wistar rats (Yoshinari et al., 2001).

PB and DEX induced transgenic CYP2B6 expression at both mRNA and protein levels. A comparison of the extents of induction appeared to suggest that CYP2B6 protein was induced to a much greater extent than was CYP2B6 mRNA. However, whereas CYP2B6 mRNA levels were readily detected in the control group, thanks to the superior sensitivity of PCR, CYP2B6 protein (in the hemizygous TG mice studied) was near the limit of detection by the monoclonal, CYP2B6-specific antibody used. Thus, the calculated fold of induction of CYP2B6 protein by PB or DEX in the CYP2B6-humanized mice was probably inaccurate, and probably represents an overestimation. This notion is supported by the in vitro activity data (Fig. 2A), which showed folds of induction that are similar to those of CYP2B6 mRNA (Fig. 1A). The low expression level, combined with the relatively low sensitivity of the immunoblot analysis for CYP2B6 protein, also made it difficult to determine whether there is a significant sex difference in the constitutive hepatic expression level of CYP2B6 protein in the humanized mouse.

In contrast to the robust increase of in vivo cotinine formation in untreated TG/*Cyp2abfgs*-null mice compared with *Cyp2abfgs*-null mice, CYP2B6 at the uninduced level did not appear to contribute substantially to microsomal metabolism of nicotine in the humanized mice, at the substrate concentrations tested (Figs. 2A and 4A), or to nicotine clearance in vivo (Fig. 5A). The impact of transgenic CYP2B6 expression was also greater on cotinine pharmacokinetics than on nicotine clearance in PB-treated mice (Fig. 5B). The apparently differing impact of CYP2B6 expression on the clearance of nicotine and cotinine may be explained by the low levels of cotinine in the *Cyp2abfgs*-null mice, which made it easy to show increases in cotinine levels in the TG/*Cyp2abfgs*-null mice. The absence of CYP2A5, the main mouse enzyme for hepatic cotinine metabolism (Zhou et al., 2010), in the TG/*Cyp2abfgs*-null mice might also have helped to amplify the impact of an increased cotinine formation on circulating cotinine levels.

In summary, the results of this study indicated that the transgenic CYP2B6 in the CYP2B6-humanized mouse model is active toward known CYP2B6 substrates. Furthermore, hepatic expression of the *CYP2B6* transgene is highly inducible by known inducers of CYP2B6 in human liver. Thus, the TG mouse and the CYP2B6-humanized mouse models will be valuable for in vivo studies on the regulation and function of human CYP2B6.

**Acknowledgments**

The authors thank Dr. Fang Xie for assistance with liquid chromatography–tandem mass spectrometry and Dr. Rachel Tyndale of the University of Toronto and Dr. Hongbing Wang of the University of Maryland for a critical reading of the manuscript. The authors acknowledge the use of the Molecular Genetics Core facility of the Wadsworth Center, New York State Department of Health.

**Authorship Contributions**

*Participated in research design*: Liu, Li, Wu, Zhang, Ding.
*Conducted experiments*: Liu, Li, Wu, Hu, Ma.
*Performed data analysis*: Liu, Li, Hu, Ma, Ding.
*Wrote or contributed to the writing of the manuscript:* Liu, Li, Zhang, Ding.

**References**

Al Koudsi N and Tyndale RF (2010) Hepatic CYP2B6 is altered by genetic, physiologic, and environmental factors but plays little role in nicotine metabolism. *Xenobiotica* **40**: 381–392.

Binnington MJ, Zhu AZ, Renner CC, Lanier AP, Hatsukami DK, Benowitz NL, and Tyndale RF (2012) CYP2A6 and CYP2B6 genetic variation and its association with nicotine metabolism in South Western Alaska Native people. *Pharmacogenet Genomics* **22**:429–440.

Bloom AJ, Martinez M, Chen LS, Bierut LJ, Murphy SE, and Goate A (2013) CYP2B6 non-coding variation associated with smoking cessation is also associated with differences in allelic expression, splicing, and nicotine metabolism independent of common amino-acid changes. *PLoS ONE* **8**:e79700.

Chen Y, Liu HF, Liu L, Nguyen K, Jones EB, and Fretland AJ (2010) The in vitro metabolism of bupropion revisited: concentration dependent involvement of cytochrome P450 2C19. *Xenobiotica* **40**:536–546.

Corcos L (1992) Phenobarbital and dexamethasone induce expression of cytochrome P-450 genes from subfamilies IIB, IIC, and IIIA in mouse liver. *Drug Metab Dispos* **20**:797–801.

Dicke KE, Skrlin SM, and Murphy SE (2005) Nicotine and 4-(methylnitrosamino)-1-(3-pyridyl)-butanone metabolism by cytochrome P450 2B6. *Drug Metab Dispos* **33**:1760–1764.

Dickmann LJ and Isoherranen N (2013) Quantitative prediction of CYP2B6 induction by estradiol during pregnancy: potential explanation for increased methadone clearance during pregnancy. *Drug Metab Dispos* **41**:270–274.

Ding XX and Coon MJ (1990) Immunochemical characterization of multiple forms of cytochrome P-450 in rabbit nasal microsomes and evidence for tissue-specific expression of P-450s NMa and NMb. *Mol Pharmacol* **37**:489–496.

Faucette SR, Hawke RL, Lecluyse EL, Shord SS, Yan B, Laethem RM, and Lindley CM (2000) Validation of bupropion hydroxylation as a selective marker of human cytochrome P450 2B6 catalytic activity. *Drug Metab Dispos* **28**:1222–1230.

Honkakoski P, Kojo A, and Lang MA (1992) Regulation of the mouse liver cytochrome P450 2B subfamily by sex hormones and phenobarbital. *Biochem J* **285**:979–983.

Johnstone E, Benowitz N, Cargill A, Jacob R, Hinks L, Day I, Murphy M, and Walton R (2006) Determinants of the rate of nicotine metabolism and effects on smoking behavior. *Clin Pharmacol Ther* **80**:319–330.

Kawamoto T, Kakizaki S, Yoshinari K, and Negishi M (2000) Estrogen activation of the nuclear orphan receptor CAR (constitutive active receptor) in induction of the mouse Cyp2b10 gene. *Mol Endocrinol* **14**:1897–1905.

Koh KH, Jurkovic S, Yang K, Choi SY, Jung JW, Kim KP, Zhang W, and Jeong H (2012) Estradiol induces cytochrome P450 2B6 expression at high concentrations: implication in estrogen-mediated gene regulation in pregnancy. *Biochem Pharmacol* **84**:93–103.

Lamba V, Lamba J, Yasuda K, Strom S, Davila J, Hancock ML, Fackenthal JD, Rogan PK, Ring B, and Wrighton SA, et al. (2003) Hepatic CYP2B6 expression: gender and ethnic differences and relationship to CYP2B6 genotype and CAR (constitutive androstane receptor) expression. *J Pharmacol Exp Ther* **307**:906–922.

Larsen MC, Brake PB, Parmar D, and Jefcoate CR (1994) The induction of five rat hepatic P450 cytochromes by phenobarbital and similarly acting compounds is regulated by a sexually dimorphic, dietary-dependent endocrine factor that is highly strain specific. *Arch Biochem Biophys* **315**:24–34.

Lee AM, Jepson C, Shields PG, Benowitz N, Lerman C, and Tyndale RF (2007) CYP2B6 genotype does not alter nicotine metabolism, plasma levels, or abstinence with nicotine replacement therapy. *Cancer Epidemiol Biomarkers Prev* **16**:1312–1314.

Li L, Jia K, Zhou X, McCallum SE, Hough LB, and Ding X (2013) Impact of nicotine metabolism on nicotine's pharmacological effects and behavioral responses: insights from a Cyp2a(4/5)bgs-null mouse. *J Pharmacol Exp Ther* **347**:746–754.

Li L, Megaraj V, Wei Y, and Ding X (2014) Identification of cytochrome P450 enzymes critical for lung tumorigenesis by the tobacco-specific carcinogen 4-(methylnitrosamino)-1-(3-pyridyl)-1-butanone (NNK): insights from a novel Cyp2abfgs-null mouse. *Carcinogenesis* **35**:2584–2591.

Mimura M, Baba T, Yamazaki H, Ohmori S, Inui Y, Gonzalez FJ, Guengerich FP, and Shimada T (1993) Characterization of cytochrome P-450 2B6 in human liver microsomes. *Drug Metab Dispos* **21**:1048–1056.

Mo SL, Liu YH, Duan W, Wei MQ, Kanwar JR, and Zhou SF (2009) Substrate specificity, regulation, and polymorphism of human cytochrome P450 2B6. *Curr Drug Metab* **10**:730–753.

Pan J, Xiang Q, and Ball S (2000) Use of a novel real-time quantitative reverse transcription-polymerase chain reaction method to study the effects of cytokines on cytochrome P450 mRNA expression in mouse liver. *Drug Metab Dispos* **28**:709–713.

Pekthong D, Desbans C, Martin H, and Richert L (2012) Bupropion hydroxylation as a selective marker of rat CYP2B1 catalytic activity. *Drug Metab Dispos* **40**:32–38.

Pustylnyak VO, Lebedev AN, Gulyaeva LF, Lyakhovich VV, and Slynko NM (2007) Comparative study of CYP2B induction in the liver of rats and mice by different compounds. *Life Sci* **80**:324–328.

Rencurel F, Stenhouse A, Hawley SA, Friedberg T, Hardie DG, Sutherland C, and Wolf CR (2005) AMP-activated protein kinase mediates phenobarbital induction of CYP2B gene expression in hepatocytes and a newly derived human hepatoma cell line. *J Biol Chem* **280**: 4367–4373.

Ring HZ, Valdes AM, Nishita DM, Prasad S, Jacob P, 3rd, Tyndale RF, Swan GE, and Benowitz NL (2007) Gene-gene interactions between CYP2B6 and CYP2A6 in nicotine metabolism. *Pharmacogenet Genomics* **17**:1007–1015.

Shimada T, Yamazaki H, Mimura M, Inui Y, and Guengerich FP (1994) Interindividual variations in human liver cytochrome P-450 enzymes involved in the oxidation of drugs, carcinogens and toxic chemicals: studies with liver microsomes of 30 Japanese and 30 Caucasians. *J Pharmacol Exp Ther* **270**:414–423.

Turpeinen M and Zanger UM (2012) Cytochrome P450 2B6: function, genetics, and clinical relevance. *Drug Metabol Drug Interact* **27**:185–197.

Walsky RL and Obach RS (2009) Measurement of in vitro cytochrome P450 2B6 activity. *Curr Protoc Toxicol* Chapter 4:Unit4 27.

Wang H and Negishi M (2003) Transcriptional regulation of cytochrome p450 2B genes by nuclear receptors. *Curr Drug Metab* **4**:515–525.

Wang H, Faucette SR, Gilbert D, Jolley SL, Sueyoshi T, Negishi M, and LeCluyse EL (2003) Glucocorticoid receptor enhancement of pregnane X receptor-mediated CYP2B6 regulation in primary human hepatocytes. *Drug Metab Dispos* **31**:620–630.

Wang H and Tompkins LM (2008) CYP2B6: new insights into a historically overlooked cytochrome P450 isozyme. *Curr Drug Metab* **9**:598–610.

Waxman DJ, Dannan GA, and Guengerich FP (1985) Regulation of rat hepatic cytochrome P-450: age-dependent expression, hormonal imprinting, and xenobiotic inducibility of sex-specific isoenzymes. *Biochemistry* **24**:4409–4417.

Wei Y, Wu H, Li L, Liu Z, Zhou X, Zhang QY, Weng Y, D'Agostino J, Ling G, and Zhang X, et al. (2012) Generation and characterization of a CYP2A13/2B6/2F1-transgenic mouse model. *Drug Metab Dispos* **40**:1144–1150.

Yamanaka H, Nakajima M, Nishimura K, Yoshida R, Fukami T, Katoh M, and Yokoi T (2004) Metabolic profile of nicotine in subjects whose CYP2A6 gene is deleted. *Eur J Pharm Sci* **22**: 419–425.

Yamano S, Nhamburo PT, Aoyama T, Meyer UA, Inaba T, Kalow W, Gelboin HV, McBride OW, and Gonzalez FJ (1989) cDNA cloning and sequence and cDNA-directed expression of human P450 IIB1: identification of a normal and two variant cDNAs derived from the CYP2B locus on chromosome 19 and differential expression of the IIB mRNAs in human liver. *Biochemistry* **28**:7340–7348.

Yamazaki H, Inoue K, Hashimoto M, and Shimada T (1999) Roles of CYP2A6 and CYP2B6 in nicotine C-oxidation by human liver microsomes. *Arch Toxicol* **73**:65–70.

Yamazoe Y, Shimada M, Murayama N, and Kato R (1987) Suppression of levels of phenobarbital-inducible rat liver cytochrome P-450 by pituitary hormone. *J Biol Chem* **262**: 7423–7428.

Yoshinari K, Sueyoshi T, Moore R, and Negishi M (2001) Nuclear receptor CAR as a regulatory factor for the sexually dimorphic induction of CYB2B1 gene by phenobarbital in rat livers. *Mol Pharmacol* **59**:278–284.

Zanger UM and Klein K (2013) Pharmacogenetics of cytochrome P450 2B6 (CYP2B6): advances on polymorphisms, mechanisms, and clinical relevance. *Front Genet* **4**:24.

Zhang QY, Dunbar D, and Kaminsky LS (2003) Characterization of mouse small intestinal cytochrome P450 expression. *Drug Metab Dispos* **31**:1346–1351.

Zhang X, D'Agostino J, Wu H, Zhang QY, von Weymarn L, Murphy SE, and Ding X (2007) CYP2A13: variable expression and role in human lung microsomal metabolic activation of the tobacco-specific carcinogen 4-(methylnitrosamino)-1-(3-pyridyl)-1-butanone. *J Pharmacol Exp Ther* **323**:570–578.

Zhang Y, Huo M, Zhou J, and Xie S (2010) PKSolver: An add-in program for pharmacokinetic and pharmacodynamic data analysis in Microsoft Excel. *Comput Methods Programs Biomed* **99**:306–314.

Zhou X, Zhuo X, Xie F, Kluetzman K, Shu YZ, Humphreys WG, and Ding X (2010) Role of CYP2A5 in the clearance of nicotine and cotinine: insights from studies on a Cyp2a5-null mouse model. *J Pharmacol Exp Ther* **332**:578–587.

Zhu AZ, Zhou Q, Cox LS, Ahluwalia JS, Benowitz NL, and Tyndale RF (2014) Gene variants in CYP2C19 are associated with altered in vivo bupropion pharmacokinetics but not bupropion-assisted smoking cessation outcomes. *Drug Metab Dispos* **42**:1971–1977.

**Address correspondence to**: Dr. Xinxin Ding, College of Nanoscale Science and Engineering, SUNY Polytechnic Institute, 257 Fuller Road, NanoFab East, Albany, NY 12203. E-mail: xding@sunycnse.com